Heliyon 11 (2025) e42332

Contents lists available at ScienceDirect

Heliyon

journal homepage: www.cell.com/heliyon

Research article

Modulation of NCX1 expression in monocytes associates with multiple sclerosis progression

Valentina Rubino [a,1], Mariarosaria Cammarota [b,1], Chiara Criscuolo [b,c], Alessandra Cianflone [d], Marco De Martino [e,f], Valeria de Rosa [b], Francesco Esposito [g], Gianmarco Abbadessa [h], Flavia Carriero [i], Giuseppe Terrazzano [i], Paolo Chieffi [e], Simona Bonavita [h], Vincenzo Bresciamorra [b,j], Lucio Annunziato [k], Giuseppina Ruggiero [a], Francesca Boscia [b,*]

[a] *Department of Medical Translational Sciences, School of Medicine, "Federico II" University of Naples, 80131, Naples, Italy*
[b] *Department of Neuroscience, Reproductive Sciences and Dentistry, School of Medicine, "Federico II" University of Naples, 80131, Naples, Italy*
[c] *CDCD Neurology, "Federico II" University Hospital, Naples, Italy*
[d] *Clinical and Translational Research Unit, Santobono-Pausilipon Children's Hospital, 80129, Naples, Italy*
[e] *Department of Precision Medicine, University of Campania "Luigi Vanvitelli", 80138, Naples, Italy*
[f] *Department of Molecular Medicine and Medical Biotechnology, University of Naples "Federico II", Naples, Italy*
[g] *Institute of Experimental Endocrinology and Oncology (IEOS) "G. Salvatore", National Research Council (CNR), 80131, Naples, Italy*
[h] *Department of Advanced Medical and Surgical Sciences, University of Campania "Luigi Vanvitelli", 80138, Naples, Italy*
[i] *Department of Health Science, University of Basilicata, 85100, Potenza, Italy*
[j] *Multiple Sclerosis Unit, Policlinico "Federico II" University Hospital, 80131, Naples, Naples, Italy*
[k] *SDN IRCCS- Synlab SDN SpA, 80143, Naples, Italy*

ARTICLE INFO

Keywords:
NCX1 exchanger
Classical $CD14^{+}CD16^{-}$ monocytes
Intermediate $CD14^{+}CD16^{+}$ monocytes
Multiple sclerosis
RRMS
SPMS
Ca^{2+}-ATPase
Na^{+}/K^{+}-ATPase

ABSTRACT

Ionic imbalance and functional heterogeneity of monocytes play key roles in multiple sclerosis (MS) progression. A better understanding of monocyte response in the context of ionic dysregulation during MS course may have relevant implications for understanding of disease pathogenesis and treatments. The sodium calcium exchanger NCX1 influences monocyte-derived macrophages reactivity under inflammation; however, little is known about its monocyte-specific expression during MS course. By means of RT-PCR, flow cytometry, and confocal analyses, we determined the expression profiling of NCX1 exchanger in monocytes of patients during relapsing-remitting MS (RRMS) and secondary progressive MS (SPMS) course. NCX1 expression was significantly upregulated in monocytes from transitional RRMS subjects. Conversely, it was significantly reduced in all monocyte subsets after RRMS conversion to SPMS. Interestingly, NCX1 levels in monocytes significantly correlated with the percentage and growth ability of the regulatory T cell (Treg) subset, whose derangement underlies MS progression. Perturbation of transcripts encoding the Ca^{2+}-ATPase isoform 1 and 4, the Na^{+}/K^{+}-ATPase α1 subunit, and the long non-coding RNA *SLC8A1-AS1* associated with NCX1 changes in peripheral blood mononuclear cells (PBMC) during MS.

* Corresponding author. Division of Pharmacology, Department of Neuroscience, Reproductive and Dentistry Sciences, School of Medicine, "Federico II" University of Naples, Via Sergio Pansini 5, 80131, Naples, Italy.
E-mail address: boscia@unina.it (F. Boscia).
[1] Valentina Rubino and Mariarosaria Cammarota have contributed equally to this work.

https://doi.org/10.1016/j.heliyon.2025.e42332
Received 17 May 2024; Received in revised form 16 January 2025; Accepted 28 January 2025
Available online 30 January 2025

Our findings demonstrated a stage-specific dysregulation of NCX1 exchanger in monocytes during MS progression and suggested that ionic imbalance in monocytes may influence not only their functional response but also the immune regulatory network during MS course. These data may be relevant for the identification of novel biomarkers and/or therapeutic targets in MS.

Abbreviations

$CD14^+CD16^-$	classical monocytes
$CD14^+CD16^+$	intermediate monocytes
CNS	central nervous system
EDSS	expanded disability status scale
lncRNA	long non-coding RNA
MIF	mean intensity of fluorescence
MS	multiple sclerosis
NCX	Na^+/Ca^{2+} exchanger
NCX1	Na^+/Ca^{2+} exchanger type 1
NCX3	Na^+/Ca^{2+} exchanger type 3
NKA	$Na^{+/}K^+$-ATPase
PBMC	peripheral blood mononuclear cells
PMCA	Ca^{2+}-ATPase
RRMS	relapsing-remitting multiple sclerosis
SPMS	secondary progressive multiple sclerosis
Treg	regulatory T cells

1. Introduction

Multiple sclerosis (MS) is an inflammatory demyelinating disease of the central nervous system (CNS) that manifests in approximately 85 % of people with a relapsing-remitting MS (RRMS) course characterized by alternating episodes of neurological deficits and recovery. Most of RRMS patients progress, within 20–25 years, to a secondary progressive (SPMS) course characterized by the accumulation of clinically irreversible neurological deficits [1–3]. Despite significant advances in our understanding of MS pathophysiology, knowledge about the mechanisms underlying the transition of RRMS to SPMS remains incomplete and the diagnosis of a progressive disease lacks reliable biomarkers. MS therapeutics show little benefit for SPMS persons, and the development of neuroprotective and remyelinating therapies is still an unmet medical need [4,5].

Proinflammatory activity of CNS microglia- and infiltrating monocyte-derived macrophages escalates during MS progression, and significantly contribute to neurodegeneration [6,7]. In parallel, a dysfunctional ionic homeostasis in brain cells accompanies MS progression and failure of repair processes [8–10]. However, it is still unclear whether ionic dysfunction contribute to the derangement of the immune regulatory network associated with functional activities of $CD14^+CD16^-$ (classical) and $CD14^+CD16^+$ (intermediate) monocytes [11–13] and regulatory T cells (Treg). This $CD4^+$ T cell subset is involved in the negative control of immune response [14], and supports the alternatively activated M2 macrophage polarization with anti-inflammatory and remyelinating properties [15,16].

The Na^+/Ca^{2+} exchangers NCX1 and NCX3, encoded by *SLC8A1* and *SLC8A3* genes, respectively, are bi-directional membrane transporters regulating sodium and calcium homeostasis under demyelinating conditions [17,18]. Current data suggest distinct functional role for NCXs in the white matter under demyelination [19]. Whereas NCX3 is required for myelin synthesis in oligodendroglia [20–23], a dysfunctional NCX1 exchanger may contribute to calcium overload and axonal degeneration [24–27]. CNS-resident microglia and circulating monocytes predominantly expresses NCX1 [28,29], whose function influence cell reactivity under inflammation [28,30]. Nevertheless, there are no information on NCXs expressed in monocyte subtypes during MS course, neither on their functional role.

The aim of the present study was to determine the expression profiling changes of NCX1 exchanger in human peripheral blood mononuclear cells (PBMC) and monocytes during RRMS and SPMS course. Furthermore, we explored the possible interference of NCX1 levels in monocytes with the cell-mediated immune-modulation regulatory network dependent on Tregs. By employing RT-PCR, flow cytometry, and immunocytochemical analyses we revealed the preferential expression of NCX1 in monocytes during MS course and its divergent modulation during the transitional RRMS stage and after conversion from RRMS to SPMS. Next, we hypothesized that NCX1 dysregulation might be associated with changes in expression level of the functionally coupled Na^+/K^+-ATPase (NKA) and Ca^{2+}-ATPase (PMCA) pumps [31–34], or might be influenced by *SLC8A1-AS1* mRNA levels, a long non coding (lcn) regulating NCX1 [35,36]. Considering that the measurements of gene expression changes in PBMC may lead to a more robust signature of the disease and also provide a better understanding of how communication between cell types affects the overall PBMC behavior, we investigated the expression profiling of *ATP1A1*, *ATP2B1* and *ATP2B4* transcripts, encoding the NKA alpha1 subunit, PMCA1 and PMCA4 pumps, and

the lcn *SLC8A1-AS1* mRNAs in whole PBMC of different MS subjects.

Overall, the hypothesis that, during MS progression, a deregulated expression of NCX1 exchanger in monocytes associates with a derangement of the Treg dependent immune-regulatory network, as well as with a perturbed regulation of the Ca^{+2}- and Na^{+}/K^{+}-ATPase pumps has been addressed.

2. Material and Methods

2.1. Ethical statement

The study was approved by the institutional review board of the Ethics Committee of the University of Naples "Federico II" (Protocol number 334/19), and written informed consent was obtained from all patients and healthy controls prior to their inclusion in the study. All procedures were performed in accordance with the Declaration of Helsinki, as revised in 2008.

2.2. Patients

Patients and healthy controls were recruited from University of Naples Federico II and University of Campania "Luigi Vanvitelli", Naples, Italy. Laboratory work was performed at the Department of Neuroscience, Reproductive Sciences and Dentistry, and at Department of Medical translational Sciences, School of Medicine, "Federico II" University of Naples, Italy. Table 1 shows a summary of demographic and clinical characteristics of MS patients and controls included in the analyses. A set of 73 patients with MS and 41 healthy controls were compared. MS was diagnosed according the McDonald 2010 diagnostic criteria [37]. The RRMS and SPMS subtypes were defined as per clinical phenotypes given by Lublin et al. [38]; and a minimum of one year of gradual worsening was required to define SPMS. The transitional phase was defined by the MS neurologists according to the evaluation of disease activity (presence of relapse and magnetic resonance imaging (MRI) activity and recover from relapse), symptoms (persistence of motor, sensory, balance/coordination, cognitive, fatigue, sphincter dysfunction) and impact on mobility and daily activities [39]. Patients not fulfilling the Lorscheider definition for SPMS or the Lublin definition for RRMS with an EDSS score $\geq$4 were defined as transitional MS [40]. Inclusion criteria were age 18–65 years for patients and controls. Exclusion criteria included primary progressive MS, autoimmune diseases other than MS, relapses or treatment with corticosteroids within 3 months, or any infection in the previous 4 weeks. Healthy controls were recruited from medical personnel who had no history or clinical evidence of neurological, systemic inflammatory or autoimmune diseases. MS patients and healthy controls were recruited in three consecutive cohorts to perform RT-PCR studies (cohort 1), flow cytometry studies (cohort 2), confocal microscopy analyses (cohort 3). Insufficient quantity of specimen or sample degradation were responsible for different numbers of patients tested in RT-PCR studies of Fig. S1 and Fig. 5.

2.3. RT-PCR

Whole blood samples were collected in EDTA tubes, kept at room temperature and extracted within 1 h after collection. Isolated PBMCs were assessed for viability by trypan blue exclusion. A minimum of 3×10^6 cells was frozen in 400 μL Trizol reagent (Life Technologies, Grand Island, NY, USA), and stored at −80 °C for RNA analysis at a later date. Total RNA was extracted and 1 μg from each sample was reverse transcribed as described [21]. The quantity and purity of RNA extractions were determined by measuring 2 μl in a Nanodrop spectrophotometer (Nanodrop 2000, Thermo Scientific). Reference genes were selected based on their stable expression across all experimental conditions. Quantitative Real-Time PCR (qRT-PCR) experiments were carried out using CFX96 thermocycler (Bio-Rad, Hercules, CA, USA). Each PCR reaction contained 10 μl of 2 × Sybr Green (Bio-Rad), 200 nM of each primer, and 20 ng of the previously produced cDNA. The Primer-BLAST program was used to design oligonucleotides for qRT-PCR. The following primer pairs were used: *SLC8A1-Forward* 5′-AAAGAGGAAGAGGAGAGGCG-3'; *SLC8A1-Reverse* 5′-AGC TGTTAGTCCCAACCACA-3'; *SLC8A3-Forward 5′-GGATAAATATGCGCGGCTTGT SLC8A3-Reverse 5′-AGCCAAATCAAAAAGCCAATCTC; ATP1A1-Forward* 5′-GACGTC CTGGAATGAAGCAT-3';

Table 1
Multiple Sclerosis patients and healthy controls' cohort demographic and clinical characteristics.

	[a]RRMS [b]EDSS≤3	RRMS EDSS≥4	[c]SPMS	Controls
Total cohort N.	35	15	23	41
Female/Male ratio N. (%)	20/15 (57.2/42.8)	11/4 (73.3/26.7)	9/14 (37/63)	24/17 (59/41)
Age (years; mean ± [d]SD)	39.2 ± 11.8	42.74 ± 10.41	46.7 ± 10.8	40.96 ± 10.57
[e]DD (years; mean ± SD)	10.3 ± 8.6	12.2 ± 7.88	15 ± 8.34	–
[f]Moderate efficacy DMT	12 (34.3)	7 (46.6)	8 (34.8)	–
[g]High efficacy DMT	23 (65.7)	8 (34.8)	14 (65.2)	–

[a] RRMS: relapsing-remitting MS.
[b] EDSS: Expanded Disability Status Scale.
[c] SPMS: secondary-progressive MS.
[d] DD: disease duration.
[e] SD: standard deviation.
[f] Moderate efficacy Disease Modifying Therapy (DMT): Dimethyl fumarate, IFN, Teriflunomide, Glatiramer acetate.
[g] High efficacy Disease Modifying Therapy (DMT): Fingolimod, Cladribine, Rituximab, Ocrelizumab, Natalizumab.

ATP1A1-Reverse 5′-TTCAGTCTTTCCGGGTGTTC-3’; *ATP2B1-Forward* 5′-TGCAGCCATAGTATCATTGGG-3’; *ATP2B1-Reverse* 5′-AGCTCCTTCAAT CCAACCAG-3’; *ATP2B4*-Forward 5′-AAAGACCCCATGTTGCTCTC-3’; *ATP2B4-Reverse* 5′-CCCCTTCGTCATCCT-CATTG-3’; *SLC8A1-AS1-Forward* 5′-CAGTCGTGTTCGTCG CACTT-3’; *SLC8A1-AS1-Reverse* 5′-GCTGCCCGTGACGTTACCTAT-3’; *GAPDH-Forward* 5′-GGAGTCAACGGATTTGGTCGT-3’; *GAPDH-Reverse 5′-GCTTCCCGTTCTCAGCCTTGA*-3’; *G6PD-Forward* 5′-ACA-GAGTGAGCCCTTCTTCAA-3’; *G6PD-Reverse* 5′-ATAGGAGTTGCGGGCAAAG-3’. The $2^{-\Delta Ct}$ formula was used to calculate the differential gene expression, as previously described [41]. Briefly, the cycle threshold (Ct) values for each gene were normalized to the housekeeping control Ct values. The obtained data were used as negative exponent of 2.

2.4. Immunofluorescence and flow cytometry analysis

Flow cytometric immunofluorescence analysis was performed on PBMC and on peripheral blood samples. PBMC were isolated by centrifugation of peripheral blood on a Ficoll-Paque cushion (GE Healthcare, Uppsala, Sweden) gradient, as previously described [42]. The following antibodies were used: PE anti-human CD3 (BD Pharmingen, San Diego, CA, USA, clone UCHT1), PE-Cy5 anti-human CD16 (eBioscience, Carlsbad, CA, USA, clone CB16), PE-Cy7 anti-human CD14 (eBioscience, Carlsbad, CA, USA, clone 61D3), rabbit polyclonal anti-NCX1 mAb (Abgent, San Diego, CA), PE anti-FoxP3-all (eBioscience, San Diego, CA, USA, clone PCH101), PE-FoxP3-exon 2 (eBioscience, San Diego, CA, USA, clone 250D/E4), FITC-anti-human Ki-67 (BD, Franklin Lakes, NJ, USA, clone B56). For intracellular detection the fixation/permeabilization solution kit BD Cytofix-Cytoperm (BD Biosciences, Franklin Lakes, NJ, USA) or the fixation and permeabilization FoxP3 buffer kit (eBioscence, San Diego, CA, USA), were employed according to the manufacturer’s instructions. For the comparative analysis of NCX1 expression levels on monocytes, fluorescence data were expressed as ratio of mean intensity of fluorescence (MIF) value for the monocyte population and the control MIF value obtained after staining of the same cell subset with the isotype control mAb, as described [43]. Flow cytometry analysis was performed by means the ATTUNE NxT acoustic focusing cytometer (Life Technologies, Carlsbad, CA, USA). Data analysis was performed by using FlowJo Software (FlowJo, LLC, Ashland, OR, USA). Due to the very low number of non classical monocytes we observed in our samples (less than 5 %), the analyses were perfomed on classical and intermediate monocyte subsets.

2.5. Confocal analysis on PBMC and monocyte cultures

Single and triple confocal immunofluorescence procedures were perfomed on PBMC or monocytes seeded on poly-lysine pre-coated glass dishes at $1x10^6$/ml in RPMI 1640 medium [44,45]. Monocytes were obtained from PBMC by using the 1-h plastic adherence enrichment protocol [46]. Non-adherent cells were removed by thorough washing with RPMI-1640 (Thermo Fisher Scientific). The adherent cells were maintained for 5 h in a humidified atmosphere containing 5 % CO_2 at 37 C° in RPMI 1640 medium. Successful isolation of monocytes (>90 %) was verified microscopically by immunofluorescence using the conjugated anti-CD14 Alexafluor647 (1:200, Abcam) and yielded about 1200 monocyte per mm^2. This procedure was adopted to limit cell activation due to detachment and resuspension. The viability was >95 %, as assessed with propidium iodide uptake. Then, cell cultures were fixed in 4 % wt/vol paraformaldehyde in phosphate buffer for 30 min. After blocking, cells were incubated with the following antibodies for 24 h: mouse monoclonal anti-NCX1 (1:1000, Swant, Bellinzona, Switzerland), rabbit polyclonal anti-CD16 (1: 1000, Abcam), and conjugated anti-CD14 Alexafluor647 (1:200, Abcam). Cells were incubated with the corresponding fluorescence-labeled secondary antibodies (Alexa488-or Alexa594-conjugated anti-mouse or anti-rabbit IgGs). DAPI was used to stain nuclei. The coverslips and the cells were mounted with Vectashield (Vector Labs, Burlingame, CA). Images were observed using a Zeiss LSM 700 laser (Carl Zeiss) scanning confocal microscope. Images were taken with an optical thickness of 0.7 μm and a resolution of 1024 × 1024. All staining and morphological analyses were blindly conducted.

NCX1 fluorescence intensity was quantified in terms of pixel intensity using Image J software, as previously described [45,47]. Images were collected at 40 × or 60 × oil immersion objective lens keeping identical laser power settings and exposure times for all photographs from each experimental set.

The intensity of CD16 and NCX1 fluorescence along plasma membrane was measured in labeled cells not touching neighboring cells. The images were contrast enhanced for optimal detection embody shape. To improve visualization, images were first thresholded and then converted to binary images. A line scan along the perimeter of the cell labeled with NCX1 or CD16 antibodies was drawn using the free hand selection tool generated using Image J software. Fluorescence intensity along the cell perimeter was determined from the non inverted images by using the plot profile plug-in and the area to line option. The number of NCX1 positive cells in PBMC cultures was determined by manual counting. Sevent to eight non-overlapping random region of interest (ROI) per slide were acquired from each patient ($n = 3$). Data from each patient were performed in duplicate and at minimum of 200 cells were counted at each condition. The average of all ROI in individual patients was used as the representative value. Measurements were made blind to the experimental group.

2.6. Statistical analysis

The statistical evaluation of data was performed with the non-parametric Mann-Whitney test Spearman’s correlation test, or simple linear regression by using GraphPad Prism 6.0 software (GraphPad Software, Inc, La Jolla, CA, USA). The data are expressed as the mean ± S.E.M of the values obtained from individual experiments. Sample size were indicated in the figure legends. Two-sided p values less than 0.05 were considered significant. A single, double or triple asterisks were used to indicate $p < 0.05$, $p \leq 0.01$ or $p \leq 0.001$ values, respectively.

3. Results

3.1. NCX1 transcripts levels decreased in PBMC from secondary progressive MS donors

To investigate the expression profiling of *SLC8A1* and *SLC8A3* genes, encoding NCX1 and NCX3 exchangers respectively, mRNA was isolated from PBMC of healthy controls, RRMS and SPMS donors, and transcripts were analyzed by RT-PCR. As showed in Fig. S1, no significant changes in *SLC8A3* transcripts were found in PBMC from RRMS or SPMS patients, when compared to healthy controls (Fig. S1, B). Conversely, *SLC8A1* transcripts were significantly reduced in PBMC isolated from SPMS, when compared to healthy subjects (Fig. S1, C). Accordingly, confocal immunofluorescence analysis revealed a significant reduction of NCX1 fluorescence intensity and NCX1-positive cells in PBMC isolated from SPMS donors when compared to healthy controls (Fig. S1, D-F). To note, confocal analysis performed on PBMC from healthy controls revealed NCX1 immunosignal in round cells with kidney-shaped nucleus, resembling a monocyte-like morphology (Fig. S1, c).

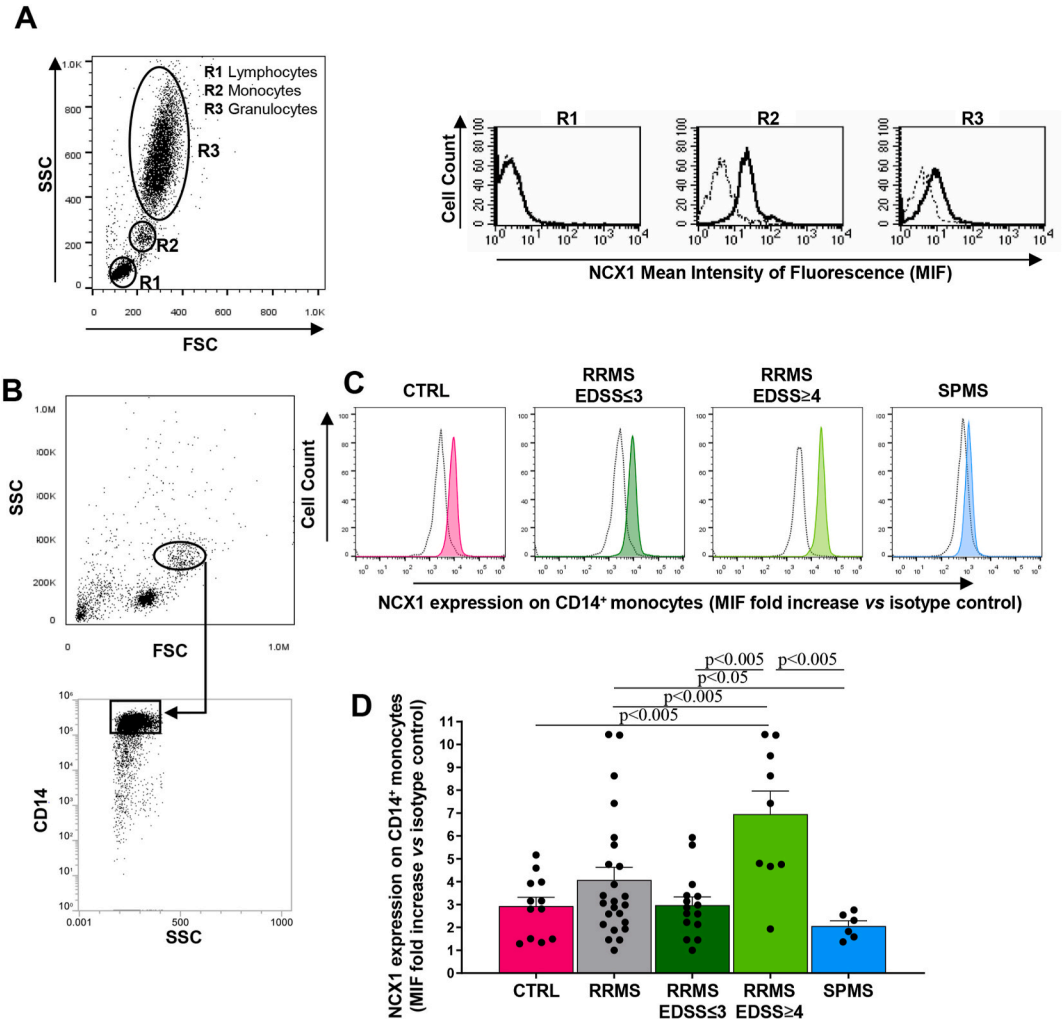

Fig. 1. Expression profiling of NCX1 in MS subjects and healthy controls. **A,** *left panel*; Flow cytometry of peripheral blood from a representative healthy control showing the gating strategy to identify lymphocytes (R1), monocytes (R2) and granulocytes (R3); *right panels* show NCX1 staining profile (bold line) in R1, R2 and R3 regions, as indicated; isotype control staining is shown as plain line; **B**, Flow cytometry from a representative healthy control showing the gating strategy to identify $CD14^+$ monocytes. **C,** NCX1 staining profile in $CD14^+$ monocytes from a representative healthy control (magenta), RRMS with EDSS≤3 (dark green), RRMS with EDSS≥4 (light green) and SPMS subject (blue); the dotted line shows the isotype control staining; **D,** Cumulative analysis of NCX1 expression on $CD14^+$ monocytes from healthy controls (CTRL, magenta column), total RRMS (grey column), RRMS with EDSS ≤3 (dark green column), RRMS with EDSS≥4 (light green column) and SPMS (blue column) subjects. NCX1 expression in $CD14^+$ monocytes has been evaluated as MIF fold increase respect to isotype control staining in the same population. Data are the means ± SEM. CTRL, n = 12; total RRMS n = 24; RRMS with EDSS ≤3, n = 15; RRMS with EDSS ≥4, n = 9; SPMS n = 6. Two-tailed Mann Whitney test; *$p < 0.05$; **$p \leq 0.01$; ***$p \leq 0.001$.

3.2. NCX1 protein increased in intermediate monocytes from transitional RRMS donors

Then, we investigated NCX1 protein expression and distribution in circulating leukocyte subsets. Flow cytometry analysis of circulating leukocytes revealed the preferential expression of NCX1 protein in monocytes (R2 region) from healthy controls (Fig. 1A). Therefore, we explored NCX1 expression in whole $CD14^+$ blood monocytes, including both the $CD14^+CD16^-$ and the $CD14^+CD16^+$

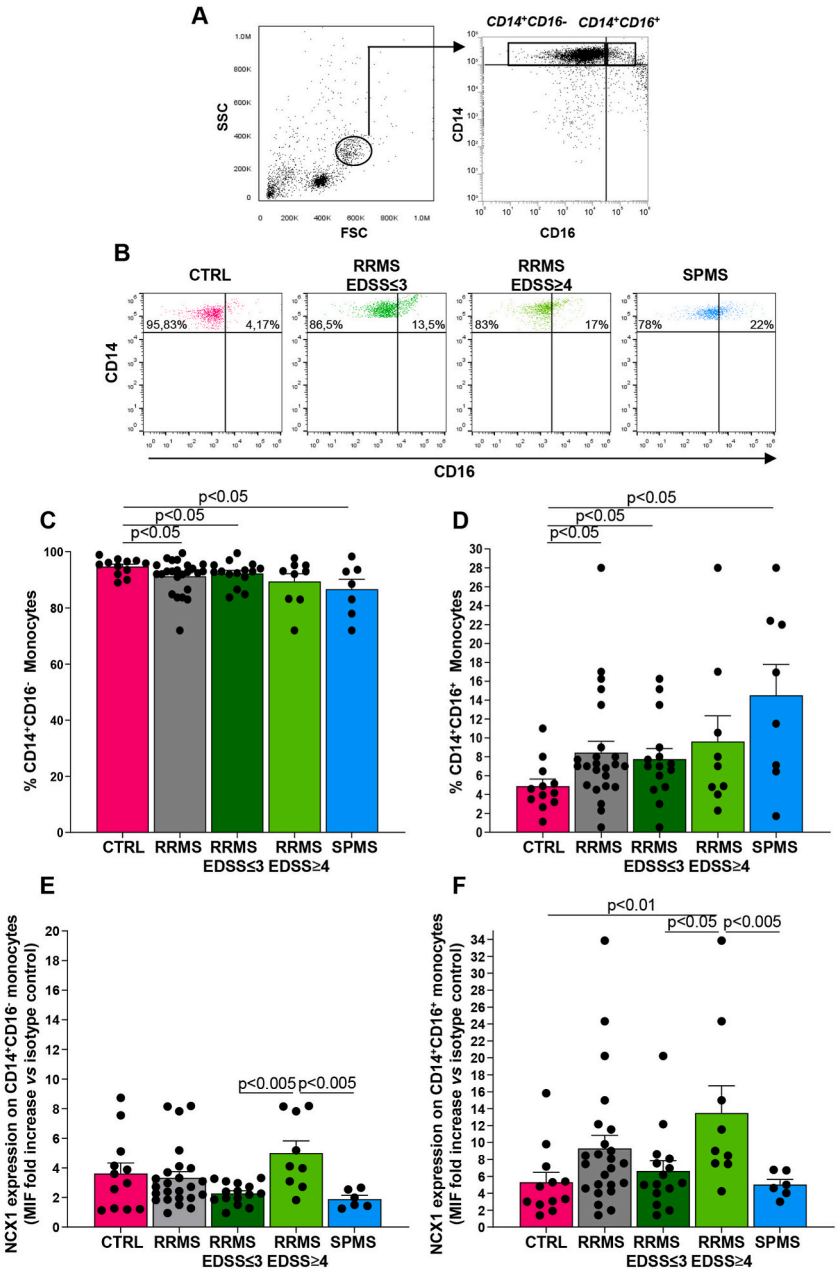

Fig. 2. NCX1 expression in monocyte subpopulations from MS donors. A, Flow cytometry plots showing the gate strategy to identify $CD14^+CD16^-$ and $CD14^+CD16^+$ monocytes in a representative healthy control. **B**, Flow cytometry plots showing the percentage of $CD14^+CD16^-$ and $CD14^+CD16^+$ monocytes in a representative healthy control (CTRL magenta), RRMS with EDSS $\leq$3 (dark green), RRMS with EDSS$\geq$4 (light green) and SPMS (blue) subject. **C-D,** Cumulative analysis of the amount of circulating $CD14^+CD16^-$ (C) and $CD14^+CD16^+$ (D) monocyte subsets in healthy controls (CTRL, magenta column), total RRMS (grey column), RRMS with EDSS $\leq$3 (dark green column), RRMS with EDSS$\geq$4 (light green column) and SPMS (blue column) subjects. **E-F**, Cumulative quantitative analysis of NCX1 expression in $CD14^+CD16^-$ (E) and $CD14^+CD16^+$ (F) monocytes from healthy controls (CTRL, magenta column), whole RRMS cohort (grey column), RRMS with EDSS $\leq$3 (dark green column), RRMS with EDSS$\geq$4 (light green column) and SPMS (blue column). Data are the means $\pm$ SEM. CTRL n = 12; total RRMS n = 24; RRMS with EDSS $\leq$3 n = 15, RRMS with EDSS $\geq$4 n = 9; SPMS n = 6. Two-tailed Mann Whitney test; *p $<$ 0.05; **p $\leq$ 0.01; ***p $\leq$ 0.001.

subsets, from healthy controls, RRMS, and SPMS donors (Fig. 1B). To better discriminate NCX1 levels in monocytes during RRMS course, donors were stratified according to their disability status, as evaluated by using the EDSS index, to include RRMS with EDSS≤ 3.0 (with moderate disability), and transitional RRMS with EDSS ≥4.0 (with higher disability). The RRMS group included both RRMS patients with EDSS ≤3 and transitional RRMS with EDSS ≥4. As showed in Fig. 1C and D, NCX1 protein levels in monocytes were not significantly different among healthy controls, total RRMS subjects and RRMS donors with EDSS ≤3. Conversely, NCX1 protein levels significantly increased in monocytes from RRMS donors with EDSS ≥4, when compared to healthy controls and the other RRMS groups. Moreover, the protein exchanger levels were significantly lower in SPMS monocytes when compared to either RRMS with EDSS ≥4 or the whole RRMS cohort.

In light of the evidence supporting an important role of intermediate $CD14^+CD16^+$ monocytes in the pathophysiology of autoimmune diseases, including MS [12], we investigated whether dysregulated NCX1 levels may be ascribed to a specific monocyte subset during MS course. To this aim, we first analyzed the percentage of classical $CD14^+CD16^-$ and intermediate $CD14^+CD16^+$ monocytes in MS donors at different disease stages (Fig. 2). Flow cytometry showed a decreasing trend of classical monocyte counts during MS

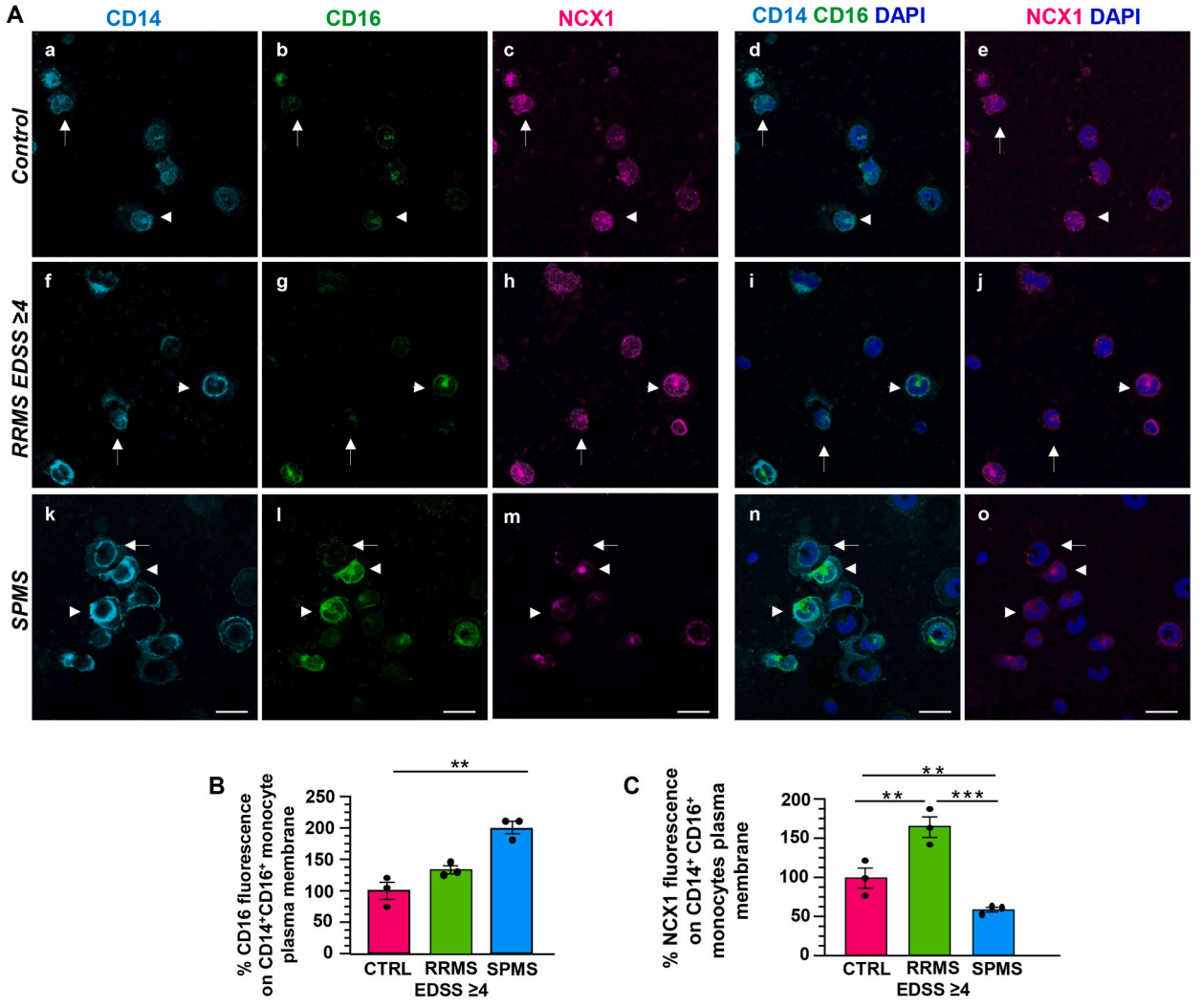

Fig. 3. Distribution of NCX1 immunoreactivity in monocytes from transitional RRMS and SPMS donors. A, Representative images of confocal triple immunofluorescence analysis displaying the co-expression of NCX1 expression (magenta) with CD14 (cyan) and CD16 (green) markers on monocyte cultures from healthy controls (a–e), RRMS with EDSS≥4 (f–j) and SPMS (k–o) donors. The cell nucleus is stained with DAPI (blue). The co-expression of CD14, CD16, and DAPI and those of NCX1 with DAPI are showed in panels d, i, n and e, j, o, respectively. Arrows point to NCX1 expression in classical $CD14^+CD16^-$ monocyte subsets. Arrowheads point to NCX1 expression in intermediate $CD14^+CD16^+$ monocytes. Note the internalized NCX1 immunosignal in double-labeled monocytes with bright $CD14^+$ and $CD16^+$ plasma membrane immunoreactivities in cultures from SPMS donors (k–o). Scale bars: 20 μm. **B-C,** Quantitative analysis of CD16 (B) and NCX1 (C) surface fluorescence intensities (at plasma membrane) on $CD14^+CD16^+$ monocyte cultures from healthy controls, RRMS with EDSS ≥4, and SPMS donors. Data were normalized as percentage of controls. The values represent the mean ± S.E.M. of the data obtained from three independent patients in each group (n = 3). Statistical significance was determined by Mann-Whitney test $p < 0.05$; **$p \leq 0.01$; ***$p \leq 0.001$.

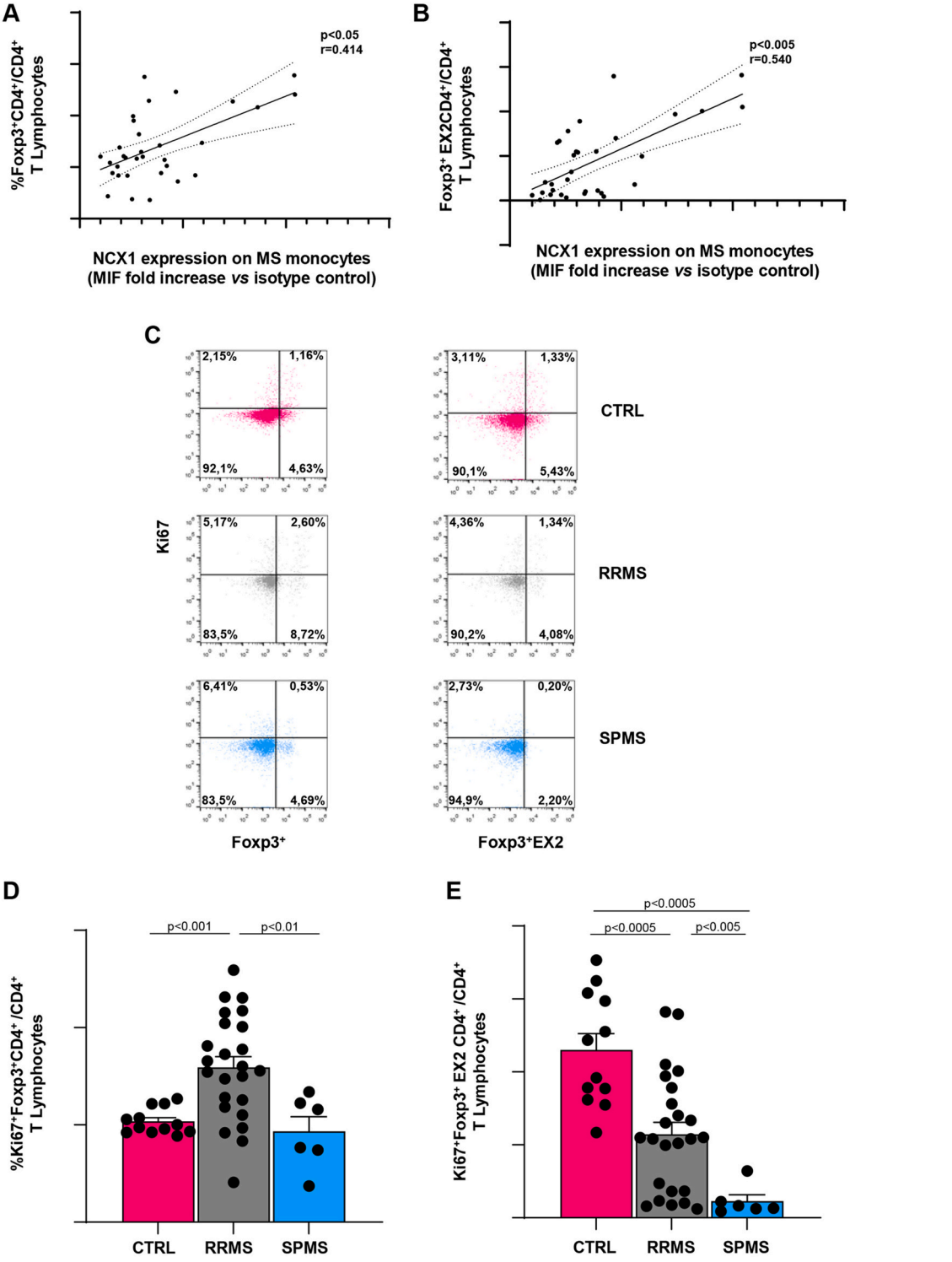

(caption on next page)

Fig. 4. Correlation of circulating Treg percentage with NCX1 expression level in monocytes of MS subjects. **A**, Correlation, as evaluated by Spearman's test, between the percentage of circulating Treg and NCX1 expression levels in monocytes of the whole MS cohort. **B**, Correlation between the percentage of circulating Treg expressing the Exon2 of the Foxp3 transcription factor and NCX1 expression levels in monocytes of the whole MS cohort. **C**, Flow cytometry plots indicating the percentage of ki67 and Foxp3 transcription factor on $CD4^+$ T lymphocytes (*left panels*) and the percentage of ki67 and Foxp3Ex2 transcription factor on $CD4^+$ T lymphocytes (*right panels*) in a representative healthy control (magenta columns), RRMS (grey columns) and SPMS (blue columns) subject. **D-E**, Cumulative analysis of the growth ability, as represented by the expression of the ki67 molecule in the Treg subset expressing the Foxp3 transcription factor (D) or in Treg cells expressing the exon 2 of the Foxp3 (E) in healthy controls (magenta columns), total RRMS (grey columns) and SPMS (blue columns) subjects. NCX1 expression in $CD14^+$ monocytes has been evaluated as MIF fold increase respect to isotype control staining in the same population. Data are the means ± SEM. CTRL, n = 12; total RRMS n = 24; SPMS n = 6. Two-tailed Mann Whitney test; *p < 0.05; **p ≤ 0.01; ***p ≤ 0.001.

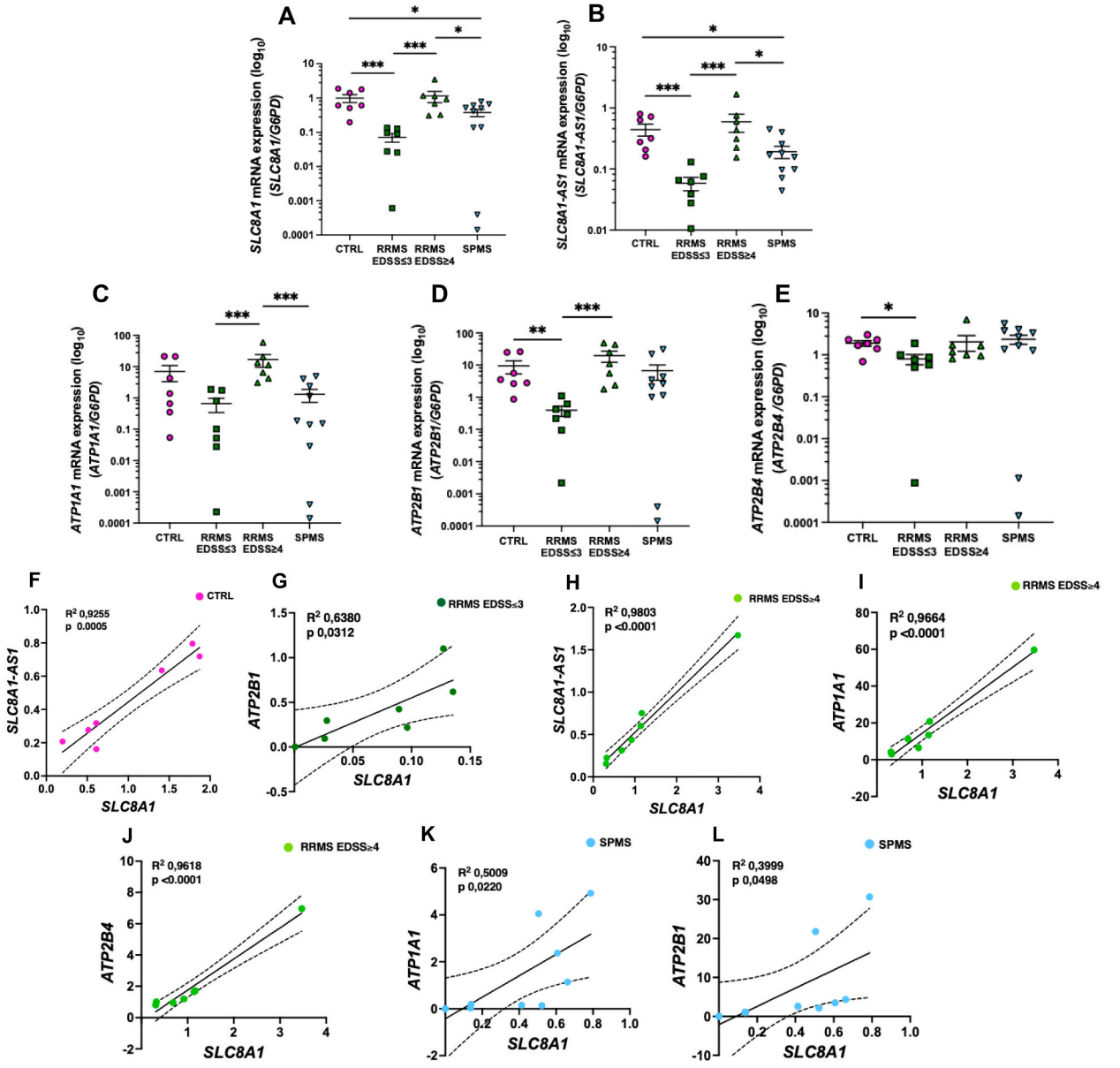

Fig. 5. mRNA profiling expression of *SLC8A1*, *ATP1A1*, *ATP2B1*, *ATP2B4*, and *lncRNA SLC8A1-AS1* in PBMC from MS donors. **A-E**, Expression levels of *SLC8A1* (A) *SLC8A1-AS1* (B) *ATP1A1* (C), *ATP2B1* (D), *ATP2B4*, (E) mRNAs in PBMC derived from MS patients and healthy subjects. Transcripts levels were plotted according to the relative expression (2-ΔCt method) measured in PBMC from healthy controls (CTRL, n = 8), RRMS with EDSS ≤3 (n = 7); RRMS with EDSS ≥4 (n = 7) and SPMS subjects (n = 10). Two-tailed Mann-Whitney test; *p < 0.05; **p ≤ 0.01; ***p ≤ 0.001. **F-I,** Scatter plot of *SLC8A1* vs. *SLC8A1-AS1* in healthy controls (F), *SLC8A1* vs. *ATP2B1* in RRMS with EDSS ≤3 (G), *SLC8A1* vs. *SLC8A1-AS1* (H), *ATP1A1* (I), and *ATP2B4 (J)* in RRMS with EDSS ≥4, and *SLC8A1* vs. *ATP1A1* (K) and *ATP2B1* (L) in SPMS. Data points indicate individual patients; the black line indicates the linear regression line.

progression. Conversely, the percentage of intermediate $CD14^+CD16^+$ monocytes increased in RRMS donors, and more so, in SPMS subjects (Fig. 2A–D). Despite this trend of increase, the absence of statistical significance in the RRMS group with EDSS $\geq$4 may result from the limited number of samples. Analysis of NCX1 levels showed no significant changes in both classical $CD14^+CD16^-$ and intermediate $CD14^+CD16^+$ monocyte subsets from RRMS donors with EDSS $\leq$3, when compared to healthy controls (Fig. 2E and F). By contrast, a significant increase in NCX1 expression was measured in both monocyte subsets from RRMS subjects with EDSS $\geq$4, if compared to both RRMS with EDSS $\leq$3 and SPMS groups. In intermediate $CD14^+CD16^+$ monocytes, the levels of NCX1 were significantly higher if compared to healthy controls (Fig. 2E and F). Conversely, both classical $CD14^+CD16^-$ and intermediate $CD14^+CD16^+$ monocytes from SPMS donors displayed reduced NCX1 protein levels if compared to RRMS group with EDSS $\geq$4 (Fig. 2E and F). No significant difference in NCX1 expression were observed between classical and intermediate monocytes from healthy controls.

These results demonstrated that NCX1 levels were upregulated in monocytes, particularly in the intermediate subsets, during the transitional RRMS stage, while they were reduced at the SPMS stage.

Next, to confirm flow cytometry data, we performed confocal triple immunofluorescence analysis with anti-NCX1, anti-CD14 and anti-CD16 antibodies in monocyte cultures obtained from transitional RRMS with EDSS $\geq$4 and SPMS donors, and analyzed both NCX1 and CD16 immunofluorescence signals along the cell plasma membrane. NCX1 immunosignal was detected in both $CD14^+CD16^-$ (arrows) and $CD14^+CD16^+$ (arrowheads) subsets isolated from healthy controls (Fig. 3A). The fluorescence intensity analysis revealed the increased CD16 expression along the plasma membrane of intermediate monocytes from SPMS patients, if compared to healthy controls (Fig. 3A and B). Interestingly, whereas NCX1 plasma membrane immunoreactivity was significantly higher in $CD14^+CD16^+$ monocytes from RRMS donors with EDSS $\geq$4, it was reduced in those from SPMS subjects, when compared to both RRMS with EDSS $\geq$4 and healthy controls (Fig. 3C). NCX1 immunosignal was scarcely detected or internalized in both $CD14^+CD16^-$ and $CD14^+CD16^+$ subsets from SPMS donors (Fig. 3A–C).

3.3. NCX1 levels in monocytes significantly correlated with the percentage of circulating regulatory T cells (Treg) in MS subjects

Cell-mediated immune-modulation dependent on Treg subset represents a key element in the control of MS pathogenesis/progression [48–50]. Moreover, the expression of the exon 2 of the Foxp3 transcription factor (Foxp3-E2) has been largely associated with effective immune suppression [51,52]. Based on these observations, we investigated the relationships between NCX1 levels on monocytes and the percentage of circulating Tregs expressing Foxp3 or Foxp3-E2 in MS subjects. With the aim to investigate the possible interference of NCX1 protein levels in MS monocytes on the general mechanisms involved in immune tolerance control, the RRMS group was examined as a whole. A significant positive correlation was observed between NCX1 expression on monocytes and the percentage of Treg lymphocytes expressing the Foxp3 transcription factor (Fig. 4A), as well as those expressing the Foxp3-E2 (Fig. 4B). To explore whether changes in Treg levels might be due to their enhanced growth ability, we evaluated the ki67 proliferation marker expression (Fig. 4C–E). A significant growth rate increase was detected in Tregs from the total RRMS group, if compared to both healthy and SPMS donors; no difference was observed between healthy controls and SPMS subjects. Conversely, and in line with previous findings [51], the growth rate of Treg lymphocytes expressing the Foxp3-E2 significantly decreased in both RRMS and SPMS groups (Fig. 4E). These findings suggest that NCX1 levels in circulating monocytes might be considered a relevant element for Treg differentiation regardless their expression of Foxp3E2 in MS subjects.

Table 2
Linear regression analysis between *SCL8A1* and associated regulatory molecules in healthy controls and MS patients.

Patients	*Gene*	$f(x)$	R^2	*P-value*
Controls	*SLC8A1-AS1*	Y = 0.3757*X + 0.06916	0.9255	**0.0005**
	ATP1A1	Y = 8.790*X - 1.755	0.3644	0.1512
	ATP2B1	Y = 11.12*X - 1.606	0.4605	0.0937
	ATP2B4	Y = 0.1174*X + 1.783	0.01119	0.8214
RRMS	*SLC8A1-AS1*	Y = 0.4093*X + 0.02923	0.3162	0.1888
EDSS≤3	*ATP1A1*	Y = 8.835*X + 0.02281	0.3195	0.1861
	ATP2B1	Y = 5.579*X - 0.007253	0.6380	**0.0312**
	ATP2B4	Y = 5.741*X + 0.3882	0.2835	0.2186
RRMS	*SLC8A1-AS1*	Y = 0.4744*X + 0.05007	0.9803	**<0.0001**
EDSS≥4	*ATP1A1*	Y = 17.97*X - 3.565	0.9664	**<0.0001**
	ATP2B1	Y = 7.107*X + 11.59	0.1520	0.3873
	ATP2B4	Y = 1.990*X - 0.2367	0.9618	**<0.0001**
SPMS	*SLC8A1-AS1*	Y = 0.2076*X + 0.1134	0.1906	0.2072
	ATP1A1	Y = 4.568*X - 0.4250	0.5009	**0.0220**
	ATP2B1	Y = 23.37*X - 2.104	0.3999	**0.0498**
	ATP2B4	Y = 2.530*X + 1.407	0.2554	0.1580

The table shows the equation f(x), R^2 and *P*-value for each gene. The *P* values < 0.05 are highlighted in bold.

3.4. SLC8A1 transcripts levels positively correlated with ATP1A1, ATP2B4, and SLC8A1-AS1 levels in PBMC from transitional RRMS donors

Finally, we investigated the dynamics of *SLC8A1* mRNA levels in PBMC from MS patients and whether they might be correlated to transcripts changes of functionally coupled Na^+/K^+-ATPase (NKA), Ca^{2+}-ATPase (PMCA) pumps or the lcn *SLC8A1-AS1*.

RT-PCR analysis revealed that *SLC8A1*, *SLC8A1-AS1*, *ATP2B1*, and *ATP2B4* transcripts significantly decreased in PBMC from RRMS donors with EDSS ≤3, when compared to healthy controls (Fig. 5A–B, D-E). Conversely, all transcripts, except *ATP2B4*, significantly increased in transitional RRMS donors with EDSS ≥4, when compared to RRMS with EDSS ≤3 (Fig. 5A–E). *ATP1A1* transcripts were significantly reduced in PBMC from SPMS patients when compared to transitional RRMS with EDSS ≥4 (Fig. 5C). *SLC8A1* and *SLC8A1-AS1* mRNAs were significantly reduced in both RRMS with EDSS ≤3 and SPMS donors when compared to healthy controls (Fig. 5A and B).

Next, to better understand the relationship between *SLC8A1* expression changes and associated regulatory molecules in PBMC from MS donors we performed a linear regression analysis between *SLC8A1* transcripts and *ATP1A1, ATP2B1*, *ATP2B4*, and *SLC8A1-AS1* mRNA levels (Table 2). *SLC8A1* levels positively correlated with *SLC8A1-AS1* in healthy controls, with *ATP2B1* in RRMS patients with EDSS ≤3, and with *ATP1A1 and ATP2B1* in SPMS donors. Interestingly, in PBMC from transitional RRMS patients with EDSS ≥4, *SLC8A1* levels positively correlated with *ATP1A1*, *ATP2B4*, and *SLC8A1-AS1* levels (Fig. 5F-L).

These findings indicated that a perturbation of transcripts encoding the PMCA1 and PMCA4 pumps, the NKA alpha1 subunit, and the *SLC8A1-AS1* mRNAs accompanied the stage-specific NCX1 dysregulation during MS.

4. Discussion

The present study shows that NCX1 exchanger expression is significantly dysregulated in blood monocytes during MS progression. Our analyses revealed divergent changes of NCX1 during the transitional RRMS phase and after SPMS conversion. More specifically, whereas NCX1 protein increased in both classical and intermediate monocyte subsets from transitional RRMS donors with EDSS ≥4, a downregulated exchanger expression was found in monocytes from SPMS patients. Perturbation of NCX1 transcript levels in PBMC was accompanied by an altered expression profiling of the ion transport *ATP1A1*, *ATP2B1*, and *ATP2B4* genes and of the lncRNA *SLC8A1-AS1* mRNAs during MS stages.

Our initial RT-PCR and flow cytometry studies showed that NCX1 levels were expressed in PBMC, particularly in blood monocytes of healthy controls, a subpopulation representing around 4–10 % of circulating PBMC. This observation may explain why a limited number of NCX1-positive cells were observed in our confocal studies on PBMC cultures. A more detailed analysis revealed that NCX1 protein levels were unchanged in monocytes from RRMS with moderate disability (EDSS ≤3), while they significantly increased in those from transitional RRMS patients with EDDS ≥4. The heterogeneity of NCX1 levels in this latter group might reflect the diverse biological characteristics of transitional patients. Nevertheless, these findings suggest that NCX1 signalling may be relevant for monocyte activities during SPMS conversion, a phase characterized by exhausting compensatory mechanisms and clinically apparent deterioration in cognitive, motor and autonomous functions [53]. Previous findings from our and other research groups have provided evidence that NCX1 is expressed in both circulating and CNS resident myeloid cells, i.e. monocytes and microglia, and upregulated by inflammatory stimuli [20,28,29]. In microglia-macrophages the upregulated NCX1 signalling regulates cell activation, migration, and phagocytosis-stimulated respiratory burst [28,54–56]. More recently, Neurobert et al. [30] pointed to NCX1 signalling as an important ionic mechanism to sense increased Na^+ levels in monocyte/macrophages, and showed that NCX1 function is required for Na^+-dependent increase of the proinflammatory activity. Although the molecular event leading to NCX1 increase and its functional role during RRMS conversion to SPMS remains to be clarified, we showed that NCX1 levels at this stage significantly increased within classical ($CD14^+CD16^-$) and intermediate ($CD14^+CD16^+$) monocytes. Compelling data indicate that such monocyte subsets represent distinct developmental stages, with the intermediate subset being the direct intermediary link between the immature classical and the more mature non classical monocyte subsets [57]. It is of relevance that intermediate monocytes, a subtype that expand during MS course, is a more active inducer of inflammation and has a direct role in neuronal damage [58,59]. In accordance, we found that $CD14^+CD16^+$ monocytes expanded during disease course, particularly at SPMS stage, a time point coinciding not only with the reduction of NCX1 levels in PBMC and monocytes, but also with increased sodium levels in MS brain [8–10]. In line, our confocal analysis showed that NCX1 immunoreactivity significantly decreased at plasma membrane level in intermediate SPMS monocytes, if compared to both RRMS with EDSS ≥4 group and healthy controls. The fact that, however, it was still observed within the cytosol may possibly explain why in flow cytometry studies the decreased levels of NCX1 did not reached the statistical significance if compared to healthy controls.

These findings not only suggest that NCX1 may contribute to monocyte heterogeneity and inter-subset plasticity during MS progression [58], but also that its reduction might be relevant for MS progression.

In line with this observation, we found a positive correlation of NCX1 expression in monocytes with the percentage of Treg lymphocytes, the immune modulating T cell subset responsible for restraining excessive inflammation and whose frequency decreases after conversion to SPMS [48]. Such T cell subset regulates effector cells in terms of clonal expansion, differentiation, cytokine profile and tissue migration. Treg also acts at level of T/dendritic cell interaction during the antigen-priming in the lymphoid organs also inhibiting the immune response in peripheral tissues [60]. Moreover, Treg-dependent suppressor activity significantly correlates with the expression of the exon 2 of Foxp3-E2 [51,52]. Accordingly, we observed a clear decrease in Treg growth ability in MS subjects, preferentially affecting the Treg lymphocytes expressing the Foxp3E2, largely associated with effective immune-modulating activity. Cytokine microenvironment, physiologically dependent on multiple immune populations, including monocytes, has been described to

interfere with Treg differentiation [61,62]. Previous studies have shown that NCX1 signalling is able to activate nuclear factor of activated T-cells 5 (NFAT-5)- dependent pathways in myeloid cells and influence pro-inflammatory TNFα production in monocytes [29,30]. Based on these observations, our findings propose that NCX1 imbalance in monocytes may participate to the deranged pro-inflammatory cytokine control pathogenetically relevant for MS progression. Although further studies are required to investigate the mechanistic link between NCX1 levels in monocytes and Treg differentiation, by us consistently found, it is possible to speculate that dysfunctional NCX1 and/or ion pumps in monocytes, by influencing sodium and calcium homeostasis may interfere with monocyte-dependent cytokine production, likely affecting Treg differentiation. These phenomena have been proposed to influence the molecular/cellular network regulating peripheral immune tolerance. In support, a recent study showed that increased sodium levels induce a pro-inflammatory signature and Treg dysfunction [63]. Considering the critical role of NCX activity in pain response [64,65], it would be interesting to investigate NCX1 expression on dorsal root ganglion and spinal cord regions of MS patients. Consistent with the differential expression of NCX1 during MS course, previous studies have shown that brain NCX1 was largely co-expressed with Nav1.6 channels in β-amyloid precursor protein APP^{+} neuronal axons of acute post-mortem SPMS lesions. Conversely, it was not found in demyelinated axons of chronic SPMS lesions [66]. These findings support the hypothesis that energy consumption over time may contribute to altered distribution of NKA and NCX1 in degenerating axons finally leading to their failure in chronic lesions of SPMS brain [67]. In line, our data showed that transcripts encoding both NCX1 and the NKA alpha1 subunit declined in PBMC after conversion to SPMS. Interestingly, emphasizing the critical role of ionic imbalance for disease progression [8–10], we found that the transcripts encoding NCX1, the plasma membrane Ca^{+2}-ATPAse PMCA1 and PMCA4 subtypes decreased in PBMC from RRMS donors with EDSS $\leq$3. These findings suggest that a reduced expression and/or activity of calcium-regulating plasma membrane transporters during RRMS course may alter the ionic gradient and indirectly influence NCX1 expression and activity at the transitional stage. The positive correlation we found between the increased *SLC8A1* transcripts levels and associated regulatory molecules at this transitional stage further support this hypothesis and highlights the importance of ionic dysregulation in PBMC during MS progression.

Although an altered NCX function in neurons and oligodendrocytes might be more critical than those in PBMC, it should be considered that infiltrating PBMC influence key functions of resident microglia-macrophages, such as removal of tissue and myelin debris, propagation of inflammation, and myelin repair, thus having subsequent effects on other CNS cells [68]. In progressive MS, the peripheral myeloid, along with B and T cell populations, take up residence within leptomeninges and the Virchow-Robin spaces, where complex interactions between peripheral and CNS resident cells serve to maintain these cellular aggregates and further propagate CNS injury [69]. Hence, the manipulation of peripherally monocyte-macrophages may provide a therapeutic treatment option to target resident cells during MS course, including oligodendrocytes for myelin repair [70]. Whether the reduced expression of NCX1 and ion transporters regulating calcium and sodium homeostasis contribute to the loss of critical macrophage functions likely producing an anti-inflammatory environment during MS progression remains to be answered. Similarly, further studies are needed to investigate on the concomitant role of the lcn *SLC8A1-AS1* during MS. Several evidence have shown that NCX1 downregulation can be determined by epigenetic modifications and microRNAs (miRNAs) under ischemic conditions [71,72]. Whether such modifications associate with NCX1 expression changes during MS progression remains to be explored.

Finally, there are several limitations in this study that could be addressed in future research. First, our study was performed on limited number of patients and without taking into account the sex or different disease-modifying therapies (DMTs) of MS patients, as they were randomly enrolled. In fact, this latter complex topic requires a specific experimental design which takes into account lack of randomization. In this regard, we have previously showed that glatiramer acetate is a DMT treatment that modulated Ca^{2+} homeostasis in B cells of RRMS patients [73]. Nevertheless, although we cannot exclude the possibility that NCX1 expression changes might be influenced by the different DMTs, we didn't observe any difference in NCX1 levels among subgroups of RRMS or SPMS patients under a moderate or high efficacy DMT regimen (Fig. S2).

Another limitation of our study concerns the lack of functional experiments that will be crucial for understanding the significance of NCX1 expression changes observed in our study, and how these changes influence the buffering capacity and/or ion concentration within the cells as well as inflammation and cell survival. These detailed analyses will require combined functional experiments applied to isolated PBMC, including cultures of monocyte-macrophage subtypes, from the different MS cohorts, and during the different stages of MS disease.

5. Conclusions

Collectively, our findings demonstrated a stage-specific dysregulation of NCX1 exchanger and other ion transporters regulating calcium and sodium homeostasis in PBMC of MS subjects. Furthermore, they suggest that NCX imbalance in monocytes may influence their functional response, thus affecting the regulation of the cell-mediated immune-modulating network during MS progression. These data, by providing a mechanistic insight into heterogenicity of monocytes and deranged regulation of the immune response during MS course may be relevant for the identification of novel biomarkers and/or therapeutic targets in MS.

CRediT authorship contribution statement

Valentina Rubino: Writing – review & editing, Methodology, Investigation, Formal analysis, Data curation. **Mariarosaria Cammarota:** Writing – review & editing, Methodology, Investigation, Formal analysis, Data curation. **Chiara Criscuolo:** Methodology, Investigation, Formal analysis. **Alessandra Cianflone:** Methodology, Investigation, Formal analysis. **Marco De Martino:** Methodology, Investigation, Formal analysis. **Valeria de Rosa:** Methodology. **Francesco Esposito:** Methodology, Investigation, Formal analysis. **Gianmarco Abbadessa:** Investigation. **Flavia Carriero:** Methodology. **Giuseppe Terrazzano:** Investigation. **Paolo**

Chieffi: Investigation. **Simona Bonavita:** Writing – review & editing, Investigation. **Vincenzo Bresciamorra:** Writing – review & editing, Investigation. **Lucio Annunziato:** Writing – review & editing, Resources. **Giuseppina Ruggiero:** Writing – review & editing, Investigation, Formal analysis, Data curation, Conceptualization. **Francesca Boscia:** Writing – original draft, Supervision, Investigation, Funding acquisition, Formal analysis, Data curation, Conceptualization.

Consent to participate

Written informed consent was obtained from patients for the usage of clinical data in anonymized fashion.

Author information

Valentina Rubino and Mariarosaria Cammarota have contributed equally to this work.

Data availability statement

The data presented in this study are available on request from the corresponding author.

Ethical statement

The study was approved by the institutional review board of the Ethics Committee of the University of Naples "Federico II" (Protocol number 334/19), and written informed consent was obtained from all patients and healthy controls prior to their inclusion in the study. All procedures were performed in accordance with the Declaration of Helsinki, as revised in 2008.

Funding

This work was financially supported by funding obtained under the National Recovery and Resilience Plan (NRRP), Mission 4 Component 2 Investment 1.3—Call for tender No. 341 of March 15, 2022 of the Italian Ministry of University and Research funded by the European Union—NextGenerationEU, Project code PE0000006, "A multiscale integrated approach to the study of the nervous system in health and disease" (MNESYS); "Iniziativa finanziata nell'ambito del Programma per il Finanziamento della Ricerca di Ateneo (FRA) 2024 dell'Università degli Studi di Napoli Federico II, con il contributor della Compagnia di San Paolo", to FB.

Declaration of competing interest

The authors declare that they have no conflicts of interest.

Acknowledgements

We thank Anna Lamberti for technical help. We thank all the participants involved in the present study. All authors have read the journal's authorship agreement.

Appendix A. Supplementary data

Supplementary data to this article can be found online at https://doi.org/10.1016/j.heliyon.2025.e42332.

References

[1] S.L. Hauser, J.R. Oksenberg, The neurobiology of multiple sclerosis: genes, inflammation, and neurodegeneration, Neuron 52 (1) (2006) 61–76, https://doi.org/10.1016/j.neuron.2006.09.011.
[2] M. Filippi, A. Bar-Or, F. Piehl, P. Preziosa, A. Solari, S. Vukusic, Rocca MA multiple sclerosis, Nat. Rev. Dis. Prim. 4 (1) (2018) 49, https://doi.org/10.1038/s41572-018-0050-3.
[3] H. Lassmann, Pathogenic mechanisms associated with different clinical courses of multiple sclerosis, Front. Immunol. 9 (2019) 3116, https://doi.org/10.3389/fimmu.2018.03116.
[4] I. Kleiter, I. Ayzenberg, J. Havla, C. Lukas, I.K. Penner, C. Stadelmann, R.A. Linker, The transitional phase of multiple sclerosis: characterization and conceptual framework, Mult Scler Relat Disord 44 (2020) 102242, https://doi.org/10.1016/j.msard.2020.102242.
[5] P. Iaffaldano, G. Lucisano, F. Patti, V. Brescia Morra, G. De Luca, A. Lugaresi, M. Zaffaroni, M. Inglese, G. Salemi, E. Cocco, A. Conte, D. Ferraro, S. Galgani, R. Bergamaschi, C. Pozzilli, M. Salvetti, G. Lus, M. Rovaris, G.T. Maniscalco, F.O. Logullo, D. Paolicelli, M. Achille, G. Marrazzo, V. Lovato, G. Comi, M. Filippi, M.P. Amato, M. Trojano, Transition to secondary progression in relapsing-onset multiple sclerosis: Definitions and risk factors, Mult Scler Italian MS Register 27 (3) (2021) 430–438, https://doi.org/10.1177/1352458520974366.
[6] A.F. Lloyd, V.E. Miron, The pro-remyelination properties of microglia in the central nervous system, Nat. Rev. Neurol. 15 (8) (2019) 447–458, https://doi.org/10.1038/s41582-019-0184-2.
[7] E. Kamma, W. Lasisi, C. Libner, H.S. Ng, J.R. Plemel, Central nervous system macrophages in progressive multiple sclerosis: relationship to neurodegeneration and therapeutics, J. Neuroinflammation 19 (1) (2022) 45, https://doi.org/10.1186/s12974-022-02408-y.

[8] M. Inglese, N. Oesingmann, W. Zaaraoui, J.P. Ranjeva, L. Fleysher, Sodium imaging as a marker of tissue injury in patients with multiple sclerosis, Mult Scler Relat Disord 2 (4) (2013) 263–269, https://doi.org/10.1016/j.msard.2013.03.009.

[9] W.J. Brownlee, B. Solanky, F. Prados, M. Yiannakas, P. Da Mota, F. Riemer, M.J. Cardoso, S. Ourselin, X. Golay, C. Gandini Wheeler-Kingshott, O. Ciccarelli, Cortical grey matter sodium accumulation is associated with disability and secondary progressive disease course in relapse-onset multiple sclerosis, J. Neurol. Neurosurg. Psychiatry 90 (7) (2019) 755–760, https://doi.org/10.1136/jnnp-2018-319634.

[10] F. Boscia, M.L. Elkjaer, Z. Illes, M. Kukley, Altered expression of ion channels in white matter lesions of progressive multiple sclerosis: what do we know about their function? Front. Cell. Neurosci. 15 (2021) 685703 https://doi.org/10.3389/fncel.2021.685703.

[11] L. Ziegler-Heitbrock, P. Ancuta, S. Crowe, M. Dalod, V. Grau, D.N. Hart, P.J. Leenen, Y.J. Liu, G. MacPherson, G.J. Randolph, J. Scherberich, J. Schmitz, K. Shortman, S. Sozzani, H. Strobl, M. Zembala, J.M. Austyn, M.B. Lutz, Nomenclature of monocytes and dendritic cells in blood, Blood 116 (16) (2010) e74–e80, https://doi.org/10.1182/blood-2010-02-258558.

[12] D. Chuluundorj, S.A. Harding, D. Abernethy, A.C. La Flamme, Expansion and preferential activation of the CD14(+)CD16(+) monocyte subset during multiple sclerosis, Immunol. Cell Biol. 92 (6) (2014) 509–517, https://doi.org/10.1038/icb.2014.15.

[13] H. Williams, C. Mack, R. Baraz, R. Marimuthu, S. Naralashetty, S. Li, H. Medbury, Monocyte differentiation and heterogeneity: inter-subset and interindividual differences, Int. J. Mol. Sci. 24 (10) (2023) 8757, https://doi.org/10.3390/ijms24108757.

[14] S. Sakaguchi, Naturally arising CD4+ regulatory t cells for immunologic self-tolerance and negative control of immune responses, Annu. Rev. Immunol. 22 (2004) 531–562, https://doi.org/10.1146/annurev.immunol.21.120601.141122.

[15] M.M. Tiemessen, A.L. Jagger, H.G. Evans, M.J. van Herwijnen, S. John, L.S. Taams, CD4+CD25+Foxp3+ regulatory T cells induce alternative activation of human monocytes/macrophages, Proc. Natl. Acad. Sci. U.S.A. 104 (49) (2007) 19446–19451, https://doi.org/10.1073/pnas.0706832104.

[16] Y. Dombrowski, T. O'Hagan, M. Dittmer, R. Penalva, S.R. Mayoral, P. Bankhead, S. Fleville, G. Eleftheriadis, C. Zhao, M. Naughton, R. Hassan, J. Moffat, J. Falconer, A. Boyd, P. Hamilton, I.V. Allen, A. Kissenpfennig, P.N. Moynagh, E. Evergren, B. Perbal, A.C. Williams, R.J. Ingram, J.R. Chan, R.J.M. Franklin, D. C. Fitzgerald, Regulatory T cells promote myelin regeneration in the central nervous system, Nat. Neurosci. 20 (5) (2017) 674–680, https://doi.org/10.1038/nn.4528.

[17] L. Annunziato, F. Boscia, G. Pignataro, Ionic transporter activity in astrocytes, microglia, and oligodendrocytes during brain ischemia, J. Cerebr. Blood Flow Metabol. 33 (7) (2013) 969–982, https://doi.org/10.1038/jcbfm.2013.44.

[18] F. Boscia, G. Begum, G. Pignataro, R. Sirabella, O. Cuomo, A. Casamassa, D. Sun, L. Annunziato, Na(+) -dependent ion transporters in pathophysiological conditions, Glia 64 (10) (2016) 1677–1697, https://doi.org/10.1002/glia.23030.

[19] F. Boscia, V. de Rosa, M. Cammarota, A. Secondo, A. Pannaccione, L. Annunziato, The Na^+/Ca^{2+} exchangers in demyelinating diseases, Cell Calcium 85 (2020) 102130, https://doi.org/10.1016/j.ceca.2019.102130.

[20] F. Boscia, C. D'Avanzo, A. Pannaccione, A. Secondo, A. Casamassa, L. Formisano, N. Guida, A. Scorziello, G. Di Renzo, L. Annunziato, New roles of NCX in glial cells: activation of microglia in ischemia and differentiation of oligodendrocytes, Adv. Exp. Med. Biol. 961 (2013) 307–316, https://doi.org/10.1007/978-1-4614-4756-6_26.

[21] V. de Rosa, A. Secondo, A. Pannaccione, R. Ciccone, L. Formisano, N. Guida, R. Crispino, A. Fico, R. Polishchuk, A. D'Aniello, L. Annunziato, F. Boscia, D-Aspartate treatment attenuates myelin damage and stimulates myelin repair, EMBO Mol. Med. 11 (1) (2019) e9278, https://doi.org/10.15252/emmm.201809278.

[22] D. Marangon, E. Boda, R. Parolisi, C. Negri, C. Giorgi, F. Montarolo, S. Perga, A. Bertolotto, A. Buffo, M.P. Abbracchio, D. Lecca, In vivo silencing of miR-125a-3p promotes myelin repair in models of white matter demyelination, Glia 68 (10) (2020) 2001–2014, https://doi.org/10.1002/glia.23819.

[23] M. Cammarota, V. de Rosa, A. Pannaccione, A. Secondo, V. Tedeschi, I. Piccialli, F. Fiorino, B. Severino, L. Annunziato, F. Boscia, Rebound effects of NCX3 pharmacological inhibition: a novel strategy to accelerate myelin formation in oligodendrocytes, Biomed. Pharmacother. 143 (2021) 112111, https://doi.org/10.1016/j.biopha.2021.112111.

[24] P.K. Stys, S.G. Waxman, B.R. Ransom, Ionic mechanisms of anoxic injury in mammalian CNS white matter: role of Na+ channels and $Na(^+)$-Ca^{2+} exchanger, J. Neurosci. 12 (2) (1991) 430–439, https://doi.org/10.1523/jneurosci.12-02-00430.1992.

[25] P.K. Stys, R.M. Lopachin, Mechanisms of calcium and sodium fluxes in anoxic myelinated central nervous system axons, Neuroscience 82 (1) (1998) 21–32, https://doi.org/10.1016/s0306-4522(97)00230-3.

[26] M.J. Craner, B.C. Hains, A.C. Lo, J.A. Black, S.G. Waxman, Co-localization of sodium channel Nav1.6 and the sodium-calcium exchanger at sites of axonal injury in the spinal cord in EAE, Brain 127 (Pt 2) (2004) 294–303, https://doi.org/10.1093/brain/awh032.

[27] M.J. Craner, J. Newcombe, J.A. Black, C. Hartle, M.L. Cuzner, S.G. Waxman, Molecular changes in neurons in multiple sclerosis: altered axonal expression of Nav1.2 and Nav1.6 sodium channels and Na^+/Ca^{2+} exchanger, Proc. Natl. Acad. Sci. U. S. A. 101 (21) (2004) 8168–8173, https://doi.org/10.1073/pnas.0402765101.

[28] F. Boscia, R. Gala, A. Pannaccione, A. Secondo, A. Scorziello, G. Di Renzo, L. Annunziato, NCX1 expression and functional activity increase in microglia invading the infarct core, Stroke 40 (11) (2009) 3608–3617, https://doi.org/10.1161/strokeaha.109.557439.

[29] R.I. Staiano, F. Granata, A. Secondo, A. Petraroli, S. Loffredo, A. Frattini, L. Annunziato, G. Marone, M. Triggiani, Expression and function of Na^+/Ca^{2+} exchangers 1 and 3 in human macrophages and monocytes, Eur. J. Immunol. 39 (5) (2009) 1405–1418, https://doi.org/10.1002/eji.200838792.

[30] P. Neubert, A. Homann, D. Wendelborn, A.L. Bär, L. Krampert, M. Trum, A. Schröder, S. Ebner, A. Weichselbaum, V. Schatz, P. Linz, R. Veelken, J. Schulte-Schrepping, A.C. Aschenbrenner, T. Quast, C. Kurts, S. Geisberger, K. Kunzelmann, K. Hammer, K.J. Binger, J. Titze, D.N. Müller, W. Kolanus, J.L. Schultze, S. Wagner, J. Jantsch, NCX1 represents an ionic Na^+ sensing mechanism in macrophages, PLoS Biol. 18 (6) (2020) e3000722, https://doi.org/10.1371/journal.pbio.3000722.

[31] F. Swift, N. Tovsrud, I. Sjaastad, O.M. Sejersted, E. Niggli, M. Egger, Functional coupling of alpha(2)-isoform Na(+)/K(+)-ATPase and Ca(2+) extrusion through the Na(+)/Ca(2+)-exchanger in cardiomyocytes, Cell Calcium 48 (1) (2010) 54–60, https://doi.org/10.1016/j.ceca.2010.06.006.

[32] M. Brini, E. Carafoli, The plasma membrane Ca^2+ ATPase and the plasma membrane sodium calcium exchanger cooperate in the regulation of cell calcium, Cold Spring Harbor Perspect. Biol. 3 (2) (2011) a004168, https://doi.org/10.1101/cshperspect.a004168.

[33] M.J. Shattock, M. Ottolia, D.M. Bers, M.P. Blaustein, A. Boguslavskyi, J. Bossuyt, J.H. Bridge, Y. Chen-Izu, C.E. Clancy, A. Edwards, J. Goldhaber, J. Kaplan, J. B. Lingrel, D. Pavlovic, K. Philipson, K.R. Sipido, Z.J. Xie, Na^+/Ca^{2+} exchange and Na^+/K^+-ATPase in the heart, J. Physiol. 593 (6) (2015) 1361–1382, https://doi.org/10.1113/jphysiol.2014.282319.

[34] M.P. Blaustein, V. Lariccia, D. Khananshvili, L. Annunziato, A. Verkhratsky, Multipurpose Na^+ ions mediate excitation and cellular homeostasis: evolution of the concept of Na^+ pumps and Na^+/Ca^{2+} exchangers, Cell Calcium 87 (2020) 102166, https://doi.org/10.1016/j.ceca.2020.102166.

[35] G.L. Guo, L.Q. Sun, M.H. Sun, H.M. Xu, LncRNA SLC8A1-AS1 protects against myocardial damage through activation of cGMP-PKG signaling pathway by inhibiting SLC8A1 in mice models of myocardial infarction, J. Cell. Physiol. 234 (6) (2019) 9019–9032, https://doi.org/10.1002/jcp.27574.

[36] L. He, H. Yang, X.L. Zhu, Y. Zhang, K. Lv, Knockdown of long non-coding RNA SLC8A1-AS1 attenuates cell invasion and migration in glioma via suppression of Wnt/β-catenin signaling pathways, Brain Res. Bull. 176 (2021) 112–120, https://doi.org/10.1016/j.brainresbull.2021.08.011.

[37] C.H. Polman, S.C. Reingold, B. Banwell, M. Clanet, J.A. Cohen, M. Filippi, K. Fujihara, E. Havrdova, M. Hutchinson, L. Kappos, F.D. Lublin, X. Montalban, P. O'Connor, M. Sandberg-Wollheim, A.J. Thompson, E. Waubant, B. Weinshenker, J.S. Wolinsky, Diagnostic criteria for multiple sclerosis: 2010 revisions to the McDonald criteria, Ann. Neurol. 69 (2) (2011) 292–302, https://doi.org/10.1002/ana.22366.

[38] F.D. Lublin, S.C. Reingold, J.A. Cohen, G.R. Cutter, P.S. Sørensen, A.J. Thompson, J.S. Wolinsky, L.J. Balcer, B. Banwell, F. Barkhof, B Jr Bebo, P.A. Calabresi, M. Clanet, G. Comi, R.J. Fox, M.S. Freedman, A.D. Goodman, M. Inglese, L. Kappos, B.C. Kieseier, J.A. Lincoln, C. Lubetzki, A.E. Miller, X. Montalban, P. W. O'Connor, J. Petkau, C. Pozzilli, R.A. Rudick, M.P. Sormani, O. Stüve, E. Waubant, C.H. Polman, Defining the clinical course of multiple sclerosis: the 2013 revisions, Neurology 83 (3) (2014) 278–286, https://doi.org/10.1212/WNL.0000000000000560.

[39] T. Ziemssen, C. Tolley, B. Bennett, S. Kilgariff, E. Jones, J. Pike, D. Tomic, D. Piani-Meier, R. Lahoz, A mixed methods approach towards understanding key disease characteristics associated with the progression from RRMS to SPMS: physicians' and patients' views, Mult Scler Relat Disord 38 (2020) 101861, https://doi.org/10.1016/j.msard.2019.101861.

[40] J. Lorscheider, K. Buzzard, V. Jokubaitis, T. Spelman, E. Havrdova, D. Horakova, M. Trojano, G. Izquierdo, M. Girard, P. Duquette, A. Prat, A. Lugaresi, F. Grand'Maison, P. Grammond, R. Hupperts, R. Alroughani, P. Sola, C. Boz, E. Pucci, J. Lechner-Scott, R. Bergamaschi, C. Oreja-Guevara, G. Iuliano, V. Van Pesch, F. Granella, C. Ramo-Tello, D. Spitaleri, T. Petersen, M. Slee, F. Verheul, R. Ampapa, M.P. Amato, P. McCombe, S. Vucic, J.L. Sánchez Menoyo, E. Cristiano, M.H. Barnett, S. Hodgkinson, J. Olascoaga, M.L. Saladino, O. Gray, C. Shaw, F. Moore, H. Butzkueven, T. Kalincik, MS Base Study Group, Defining secondary progressive multiple sclerosis, Brain 139 (Pt9) (2016) 2395–2405, https://doi.org/10.1093/brain/aww173.

[41] K.J. Livak, T.D. Schmittgen, Analysis of relative gene expression data using real-time quantitative PCR and the 2(-Delta Delta C(T), Methods 25 (4) (2001) 402–408, https://doi.org/10.1006/meth.2001.1262.

[42] V. Rubino, A.T. Palatucci, Rosa G. La, A. Giovazzino, F. Aruta, S. Damiano, F. Carriero, M. Santillo, R. Iodice, P. Mondola, G. Ruggiero, G. Terrazzano, Superoxide dismutase-1 intracellular content in T lymphocytes associates with increased regulatory T cell level in multiple sclerosis subjects undergoing immune-modulating treatment, Antioxidants 10 (12) (2021) 1940, https://doi.org/10.3390/antiox10121940.

[43] F. Alfinito, M. Sica, L. Luciano, R. Della Pepa, C. Palladino, I. Ferrara, U. Giani, G. Ruggiero, G. Terrazzano, Immune dysregulation and dyserythropoiesis in the myelodysplastic syndromes, Br. J. Haematol. 148 (1) (2010) 90–98, https://doi.org/10.1111/j.1365-2141.2009.07921.x.

[44] F. Boscia, C. Passaro, V. Gigantino, S. Perdonà, R. Franco, G. Portella, S. Chieffi, P. Chieffi, High levels of GPR30 protein in human testicular carcinoma in situ and seminomas correlate with low levels of estrogen receptor-beta and indicate a switch in estrogen responsiveness, J. Cell. Physiol. 230 (6) (2015) 1290–1297, https://doi.org/10.1002/jcp.24864.

[45] F. Boscia, A. Pannaccione, R. Ciccone, A. Casamassa, C. Franco, I. Piccialli, V. de Rosa, A. Vinciguerra, G. Di Renzo, L. Annunziato, The expression and activity of KV3.4 channel subunits are precociously upregulated in astrocytes exposed to Aβ oligomers and in astrocytes of Alzheimer's disease Tg2576 mice, Neurobiol. Aging 54 (2017) 187–198, https://doi.org/10.1016/j.neurobiolaging.2017.03.008.

[46] E.L. Hopewell, C. Cox, Manufacturing dendritic cells for immunotherapy: monocyte enrichment, Mol Ther Methods Clin Dev 16 (2020) 155–160, https://doi.org/10.1016/j.omtm.2019.12.017.

[47] M. Cammarota, F. Boscia, Contribution of oligodendrocytes, microglia, and astrocytes to myelin debris uptake in an explant model of inflammatory demyelination in rats, Cells 12 (17) (2023) 2203, https://doi.org/10.3390/cells12172203.

[48] F. Carbone, V. De Rosa, P.B. Carrieri, S. Montella, D. Bruzzese, A. Porcellini, C. Procaccini, A. La Cava, G. Matarese, Regulatory T cell proliferative potential is impaired in human autoimmune disease, Nat. Med. 20 (2014) 69–74, https://doi.org/10.1038/nm.3411.

[49] M. Sambucci, F. Gargano, G. Guerrera, L. Battistini, G. Borsellino, One, No one, and one hundred thousand: T regulatory cells' multiple identities in neuroimmunity, Front. Immunol. 10 (2019) 2947, https://doi.org/10.3389/fimmu.2019.02947.

[50] N.J. Booth, A.J. McQuaid, T. Sobande, S. Kissane, E. Agius, S.E. Jackson, M. Salmon, F. Falciani, K. Yong, M.H. Rustin, Different proliferative potential and migratory characteristics of human CD4+ regulatory T cells that express either CD45RA or CD45RO, J. Immunol. 184 (2010) 4317–4326, https://doi.org/10.4049/jimmunol.0903781.

[51] V. De Rosa, M. Galgani, A. Porcellini, A. Colamatteo, M. Santopaolo, C. Zuchegna, A. Romano, S. De Simone, C. Procaccini, C. La Rocca, Glycolysis controls the induction of human regulatory T cells by modulating the expression of FOXP3 exon 2 splicing variants, Nat. Immunol. 16 (11) (2015) 1174–1184, https://doi.org/10.1038/ni.3269.

[52] Y. Sato, J. Liu, E. Lee, R. Perriman, M.G. Roncarolo, R. Bacchetta, Co-expression of FOXP3FL and FOXP3Δ2 isoforms is required for optimal treg-like cell phenotypes and suppressive function, Front. Immunol. 12 (2021) 752394, https://doi.org/10.3389/fimmu.2021.752394.

[53] I. Kleiter, I. Ayzenberg, J. Havla, C. Lukas, I.K. Penner, C. Stadelmann, R.A. Linker, The transitional phase of multiple sclerosis: characterization and conceptual framework, Mult Scler Relat Disord 102242 (2020), https://doi.org/10.1016/j.msard.2020.102242.

[54] T. Nagano, Y. Kawasaki, A. Baba, M. Takemura, T. Matsuda, Up-regulation of Na(+)-Ca2+ exchange activity by interferon-gamma in cultured rat microglia, J. Neurochem. 90 (4) (2004) 784–791, https://doi.org/10.1111/j.1471-4159.2004.02511.x.

[55] E.W. Newell, E.F. Stanley, L.C. Schlichter, Reversed Na^+/Ca^{2+} exchange contributes to Ca^{2+} influx and respiratory burst in microglia, Channels 1 (5) (2007) 366–376, https://doi.org/10.4161/chan.5391.

[56] M. Ifuku, K. Färber, Y. Okuno, Y. Yamakawa, T. Miyamoto, C. Nolte, V.F. Merrino, S. Kita, T. Iwamoto, I. Komuro, B. Wang, G. Cheung, E. Ishikawa, H. Ooboshi, M. Bader, K. Wada, H. Kettenmann, M. Noda, Bradykinin-induced microglial migration mediated by B1-bradykinin receptors depends on Ca2+ influx via reverse-mode activity of the Na^+/Ca^{2+} exchanger, J. Neurosci. 27 (48) (2007) 13065–13073, https://doi.org/10.1523/jneurosci.3467-07.2007.

[57] K.L. Wong, J.J. Tai, W.C. Wong, H. Han, X. Sem, W.H. Yeap, P. Kourilsky, S.C. Wong, Gene expression profiling reveals the defining features of the classical, intermediate, and nonclassical human monocyte subsets, Blood 118 (2011) e16–e31.

[58] S.T. Gren, T.B. Rasmussen, S. Janciauskiene, K. Håkansson, J.G. Gerwien, O. Grip, A single-cell gene-expression profile reveals inter-cellular heterogeneity within human monocyte subsets, PLoS One 10 (12) (2015) e0144351, https://doi.org/10.1371/journal.pone.0144351.

[59] I. Visan, Monocytes as targets, Nat. Immunol. 23 (5) (2022) 645, https://doi.org/10.1038/s41590-022-01205-2.

[60] J. Huehn, A. Hamann, Homing to suppress: address codes for Treg migration, Trends Immunol. 26 (12) (2005) 632–636, https://doi.org/10.1016/j.it.2005.10.001.

[61] A.M. Joudi, C.P. Reyes Flores, B.D. Singer, Epigenetic control of regulatory T cell stability and function: implications for translation, Front. Immunol. 13 (2022) 861607, https://doi.org/10.3389/fimmu.2022.861607. PMID: 35309306; PMCID: PMC8924620.

[62] J.N. Khantakova, S.V. Sennikov, T-helper cells flexibility: the possibility of reprogramming T cells fate, Front. Immunol. 14 (2023) 1284178, https://doi.org/10.3389/fimmu.2023.1284178.

[63] B.F. Côrte-Real, I. Hamad, R. Arroyo Hornero, S. Geisberger, J. Roels, L. Van Zeebroeck, A. Dyczko, M.W. van Gisbergen, H. Kurniawan, A. Wagner, N. Yosef, S. N.Y. Weiss, K.G. Schmetterer, A. Schröder, L. Krampert, S. Haase, H. Bartolomaeus, N. Hellings, Y. Saeys, L.J. Dubois, D. Brenner, S. Kempa, D.A. Hafler, J. Stegbauer, R.A. Linker, J. Jantsch, D.N. Müller, M. Kleinewietfeld, Sodium perturbs mitochondrial respiration and induces dysfunctional Tregs, Cell Metabol. 35 (2) (2023) 299–315.e8, https://doi.org/10.1016/j.cmet.2023.01.009.

[64] Huang Y, Wen LL, Xie JD, Ouyang HD, Chen DT, Zeng WA. Antinociceptive effectiveness of the inhibition of NCX reverse-mode action in rodent neuropathic pain model.MolPain2019;15:1744806919864511.https://doi:10.1177/1744806919864511.

[65] T. Trendafilova, K. Adhikari, A.B. Schmid, R. Patel, E. Polgár, K.I. Chisholm, S.J. Middleton, K. Boyle, A.C. Dickie, E. Semizoglou, J. Perez-Sanchez, A.M. Bell, L. M. Ramirez-Aristegueta, S. Khoury, A. Ivanov, H. Wildner, E. Ferris, J.C. Chacón-Duque, S. Sokolow, M.A. Saad Boghdady, A. Herchuelz, P. Faux, G. Poletti, C. Gallo, F. Rothhammer, G. Bedoya, H.U. Zeilhofer, L. Diatchenko, S.B. McMahon, A.J. Todd, A.H. Dickenson, A. Ruiz-Linares, D.L. Bennett, Sodium-calcium exchanger-3 regulates pain "wind-up": from human psychophysics to spinal mechanisms, Neuron 110 (16) (2022) 2571–2587.e13, https://doi.org/10.1016/j.neuron.2022.05.017.

[66] J.A. Black, J. Newcombe, B.D. Trapp, S.G. Waxman, Sodium channel expression within chronic multiple sclerosis plaques, J. Neuropathol. Exp. Neurol. 66 (9) (2007) 828–837, https://doi.org/10.1097/nen.0b013e3181462841.

[67] E.A. Young, C.D. Fowler, G.J. Kidd, A. Chang, R. Rudick, E. Fisher, B.D. Trapp, Imaging correlates of decreased axonal Na^+/K^+ ATPase in chronic multiple sclerosis lesions, Ann. Neurol. 63 (4) (2008) 428–435, https://doi.org/10.1002/ana.21381.

[68] A.D. Greenhalgh, J.G. Zarruk, L.M. Healy, S.J. Baskar Jesudasan, P. Jhelum, C.K. Salmon, A. Formanek, M.V. Russo, J.P. Antel, D.B. McGavern, B.W. McColl, S. David, Peripherally derived macrophages modulate microglial function to reduce inflammation after CNS injury, PLoS Biol. 16 (10) (2018) e2005264, https://doi.org/10.1371/journal.pbio.2005264.

[69] S. Monaco, R. Nicholas, R. Reynolds, R. Magliozzi, Intrathecal inflammation in progressive multiple sclerosis, Int. J. Mol. Sci. 21 (21) (2020) 8217, https://doi.org/10.3390/ijms21218217.

[70] L.H. Forbes, V.E. Miron, Monocytes in central nervous system remyelination, Glia 70 (5) (2022) 797–807, https://doi.org/10.1002/glia.24111.

[71] V. Valsecchi, G. Pignataro, A. Del Prete, R. Sirabella, C. Matrone, F. Boscia, A. Scorziello, M.J. Sisalli, E. Esposito, N. Zambrano, G. Di Renzo, L. Annunziato, NCX1 is a novel target gene for hypoxia-inducible factor-1 in ischemic brain preconditioning, Stroke 42 (3) (2011) 754–763, https://doi.org/10.1161/STROKEAHA.110.597583.

[72] A. Vinciguerra, L. Formisano, P. Cerullo, N. Guida, O. Cuomo, A. Esposito, G. Di Renzo, L. Annunziato, G. Pignataro, MicroRNA-103-1 selectively downregulates brain NCX1 and its inhibition by anti-miRNA ameliorates stroke damage and neurological deficits, Mol. Ther. 22 (10) (2014) 1829–1838, https://doi.org/10.1038/mt.2014.113.

[73] C. Criscuolo, A. Cianflone, R. Lanzillo, D. Carrella, A. Carissimo, F. Napolitano, R. de Cegli, P. de Candia, C. La Rocca, T. Petrozziello, G. Matarese, F. Boscia, A. Secondo, D. Di Bernardo, V. Brescia Morra, Glatiramer Acetate modulates ion channels expression and calcium homeostasis in B cell of patients with relapsing-remitting multiple sclerosis, Sci. Rep. 9 (1) (2019) 4208, https://doi.org/10.1038/s41598-018-38152-8.